FEBS Letters 587 (2013) 3495–3499

journal homepage: www.FEBSLetters.org

Solution NMR determination of hydrogen bonding and base pairing between the *glyQS* T box riboswitch Specifier domain and the anticodon loop of $tRNA^{Gly}$ ☆

Andrew T. Chang, Edward P. Nikonowicz *

Department of Biochemistry and Cell Biology, Rice University, Houston, TX 77005-1892, United States

ARTICLE INFO

Article history:
Received 11 July 2013
Revised 30 August 2013
Accepted 2 September 2013
Available online 11 September 2013

Edited by Michael Ibba

Keywords:
Heteronuclear
U-turn
tRNA
Transcription regulation
Riboswitch
Antitermination
Difference spectrum

ABSTRACT

In Gram-positive bacteria the tRNA-dependent T box riboswitch regulates the expression of many amino acid biosynthetic and aminoacyl-tRNA synthetase genes through a transcription attenuation mechanism. The Specifier domain of the T box riboswitch contains the Specifier sequence that is complementary to the tRNA anticodon and is flanked by a highly conserved purine nucleotide that could result in a fourth base pair involving the invariant U_{33} of tRNA. We show that the interaction between the T box Specifier domain and tRNA consists of three Watson–Crick base pairs and that U_{33} confers stability to the complex through intramolecular hydrogen bonding. Enhanced packing within the Specifier domain loop E motif may stabilize the complex and contribute to cognate tRNA selection.

1. Introduction

In Gram-positive bacteria, the transcription of many tRNA synthetase genes and genes involved in amino acid metabolism is regulated in a tRNA-dependent manner by the T-box riboswitch [1,2]. The T-box riboswitch includes a 200–300 nt region of mRNA located 5′ to the translation start codon (also known as the mRNA leader region) that can form multiple conserved secondary structure elements and selectively binds gene-specific tRNA species (Fig. 1) [3]. The binding of uncharged tRNA stabilizes a 3′-proximal RNA hairpin designated the antiterminator helix and prevents premature transcription termination [4].

The Specifier domain (SD) is a structural element in the 5′ region of the mRNA leader that is variable in size and contains the Specifier sequence, three nucleotides that are complementary to the anticodon nucleotides of the cognate tRNA. The specificity of the riboswitch for tRNA is primarily achieved through pairing of the Specifier sequence nucleotides with the anticodon of tRNA [4,5] and changes in this sequence can switch the specificity of the T-box riboswitch to allow recognition of other tRNA species [4–6]. In addition to the Specifier sequence, the SD contains a loop E structural motif that is necessary for proper regulatory function and structure maintenance [7–9]. The SD also contains a highly conserved purine residue immediately 3′ to the Specifier sequence that is positioned to pair with the invariant U_{33} of tRNA [6,10], creating the potential for a fourth base pair between the anticodon loop and the Specifier loop. This residue is protected from Mg^{2+} cleavage in the tRNA–mRNA leader complex [11], supporting the possibility that the tRNA–SD interaction involves four base pairs [12]. Recent SHAPE analysis of tRNA in complex with stem I of the *Geobacillus kaustophilus glyQS* T-box riboswitch (which includes the Specifier domain) indicated protection of U_{33} but not of the conserved adenine [13]. However, in the recently reported co-crystal structure of the *Oceanobacillus iheyensis glyQ* riboswitch Stem I with $tRNA^{Gly}$, the Specifier–tRNA interaction involves three base pairs and the U_{33} of tRNA loops out [14].

We have used NMR spectroscopy and isothermal calorimetry (ITC) to examine the interaction between the anticodon arm of $tRNA^{Gly,GCC}$ (ASL^{Gly}) and the SD of the *Bacillus subtilis tyrS* mRNA

Abbreviations: NOESY, nuclear Overhauser effect spectroscopy; 2D, two dimensional; HMQC, heteronuclear multiple quantum coherence; NH, imino; CW, continuous wave; SD, specifier domain

☆ This work was supported by National Institutes of Health grant GM73969 to E.P.N.

* Corresponding author. Fax: +1 713 348 5154.
E-mail address: edn@rice.edu (E.P. Nikonowicz).

0014-5793/$36.00 © 2013 Federation of European Biochemical Societies. Published by Elsevier B.V. All rights reserved.
http://dx.doi.org/10.1016/j.febslet.2013.09.003

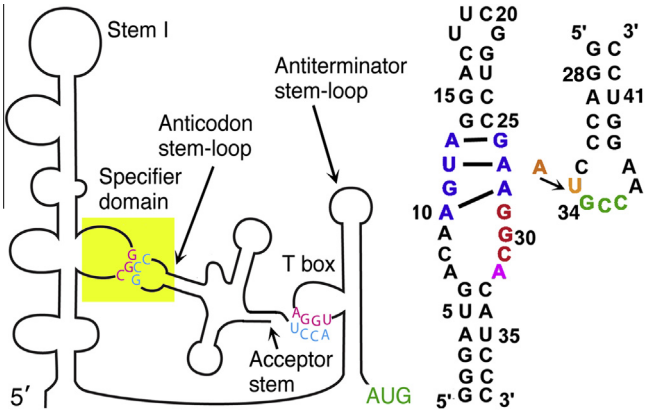

Fig. 1. (Left) Generalized secondary structure of the T box riboswitch in complex with tRNA. The domain of Stem I containing the Specifier sequence and the anticodon loop of tRNA are highlighted. (Right) The nucleotide sequences corresponding to the Specifier domain of the *tyrS* T box riboswitch with glycyl Specifier sequence GGC (*tyrS*^{GGC}) and the anticodon arm of tRNA^{Gly,GCC} (ASL^{Gly}) from *Bacillus subtilis* (tRNA numbering used for ASL^{Gly}). The Specifier (red) and anticodon (green) nucleotides confer specificity to the interaction. The highly conserved A (magenta) in the Specifier domain and the invariant U (orange) of the anticodon loop also have been proposed to pair [11]. Nucleotides of the SD that form the loop E motif are shown in blue.

leader containing the glycyl Specifier sequence, GGC. The SD–ASL^{Gly} complex is formed by three stacked intermolecular Watson–Crick G–C base pairs. The conformation of the ASL^{Gly} loop transitions from dynamic and disordered to a moderately stable U-turn structural motif in the complex. A $U_{33}A$ mutant of ASL^{Gly} that is unable to form the canonical U-turn motif retains the ability to bind SD but with reduced affinity. Our data are consistent with a configuration where the conserved purine 3′ to the Specifier sequence and the conserved purine 3′ to the anticodon (residue 37 of tRNA) stack against the ends of the intermolecular helix and may confer additional stability to the complex. These results are consistent with the co-crystal structure of the *glyQ* T box–tRNA complex and observations of solution SHAPE experiments [13,14].

2. Methods

The RNA sequences shown in Fig. 1 were prepared by in vitro transcription with T7 RNA polymerase using synthetic DNA templates and either unlabeled or $^{13}C/^{15}N$ -labeled 5′-NTPs [15]. The RNA molecules were purified using 20% (w/v) preparative polyacrylamide gels, electroeluted, and precipitated with ethanol. The RNA molecules were suspended an extensively dialyzed against 10 mM KCl and 5 mM potassium phosphate, pH 6.8. The samples were then heated to 90 °C for 60 s and snap cooled on ice before addition of $MgCl_2$ to 2.0 mM and 10% D_2O. All RNA samples were concentrated to a volume of 330 mL. The sample concentrations varied between 0.5–1.0 mM and were checked for RNA integrity using denaturing PAGE.

All NMR spectra were acquired on Varian Inova 600 and 800 MHz spectrometers equipped with cryogenically cooled ^{1}H–[^{13}C,^{15}N] probes and solvent suppression was achieved using binomial read pulses. For selectively decoupled 1D difference experiments, pairs of ^{1}H spectra were recorded with application of on- or off-resonance low power (833 Hz) continuous wave (CW) ^{15}N decoupling during acquisition. 2D ^{15}N–^{1}H HMQC spectra were collected to identify ^{15}N–^{1}H chemical shift correlations. 2D NOESY and NOESY–HMQC spectra (t_m = 180 ms) and were acquired at 16 °C to obtain sequence specific NH ^{1}H resonance assignments. Typically, the data points were extended by 25% using linear prediction for the indirectly detected dimensions. NMR spectra were processed and analyzed using Felix 2007 (Felix NMR Inc., San Diego, CA).

A VP-ITC calorimeter (MicroCal, Inc.) was used for the ITC experiments. The concentrations of RNA in the injection syringe and sample cell were 260–350 μM and 20–30 μM, respectively. Thirty 10 μL injections into 1.8 mL sample cell volume were performed at 10 °C with 5 min between injections. Control titrations (forward and reverse) were performed and yielded similar results [16]. The ITC data was analyzed using the vendor-supplied software (ORIGIN v7.0) and plots of ΔH versus mole ratio were generated from the raw thermograms. The final 4–6 points from each experiment were extrapolated to obtain a straight line that was subtracted from all the data before determining K_a (association constant) and n (reaction stoichiometry) by fitting the points using a non-liner least squares model for a single binding site.

3. Results and discussion

The SD sequence (Fig. 1) corresponds to that of the *B. subtilis tyrS* mRNA leader with the tyrosyl UAC Specifier sequence replaced by the glycyl GGC [5]. The imino (NH) resonances of the SD and ASL^{Gly} molecules were monitored using ^{15}N–^{1}H HMQC spectra (Fig. 2) and assigned using NOESY-based experiments. Preliminary studies to identify and optimize conditions that stabilize the SD–ASL^{Gly} complex demonstrated that Mg^{2+} was necessary. Addition of Mg^{2+} to ASL^{Gly} disrupts the C_{32}-A^{+}_{38} base pair of the hairpin [17,18], but has little effect on the NH spectrum (Fig. 2B). Addition of Mg^{2+} to SD reinforces the loop E motif as evidenced by the appearance of NH resonances for nucleotides U_{12} and G_{26} that participate in reverse Hoogsteen U-A and sheared A–G base pairs, respectively (Fig. 2A). The NH resonance of the bulged G_{11} nucleotide shifts 1.0 ppm upfield in response to Mg^{2+} binding. At the base of the Specifier loop, the NH resonances of U_{35}, U_5, and G_6 are doubled and the splitting is most pronounced for residues proximal to the loop–helix junction. Exchange cross peaks between the split resonances in the NOESY spectrum (not shown) are indicative of two conformations at the base of the Specifier loop.

The SD–ASL^{Gly} complexes were prepared such that one of the RNA molecules was $^{13}C/^{15}N$-labeled and the other was unlabeled. In the HMQC spectrum of SD, complex formation leads to the appearance of two additional guanine NH resonances at 11.85 ppm (G_{29}) and 13.14 ppm (G_{30}) (Fig. 2A). These resonances give rise to a cross peak in the NOESY spectrum (Fig. 2C). The resonance at 13.14 ppm also has a NOE cross peak with a NH resonance at 12.78 ppm. A ^{15}N-edited NOESY spectrum indicated this later NOE cross peak is *inter*-molecular, establishing the identities of the NH resonances at 13.14 and 12.78 ppm as G_{30} of SD and $^{*}G_{34}$ of ASL^{Gly}, respectively. Also in the complex, split SD resonances of U_{35}, U_5, and G_6 collapse into single peaks with chemical shifts unique to the complex (Fig. 2A). In the loop E motif, the U_{12} NH resonance intensifies and the G_{26} ^{15}N NH resonance shifts 4.0 ppm upfield. The shift of the G_{26} resonance is consistent with formation of the extensive hydrogen bond network involving the base O6, N1, and N2 atoms of this residue in the context of a loop E motif [19]. Together, these results indicate that binding of ASL^{Gly} imposes conformational ordering to the base of the Specifier loop and within the loop E motif.

The free form of ASL^{Gly} has a five base pair stem, but the seven nucleotide loop does not adopt the archetypal U-turn motif [17]. The ^{15}N–^{1}H HMQC spectrum contains four major peaks corresponding to the stem nucleotides and a fifth weak peak that corresponds to the terminal G_{27} (Fig. 2B). Three additional peaks in the NH ^{1}H spectrum are exchange broadened and do not give rise to peaks in the HMQC spectrum. Because there is no evidence for multiple conformations of the stem nucleotides in other ASL^{Gly} spectra, these resonances were tentatively assigned to U_{33} and